First-principles calculation of the structural, electronic, and vibrational properties of gallium nitride and aluminum nitride

K. Miwa and A. Fukumoto
Toyota Central Research & Development Laboratories, Inc., 41-1 Aza Yokomichi, Oaza Nagakute, Nagakute-cho, Aichi-gun, Aichi-ken 480-11, Japan
(Received 19 March 1993)

First-principles pseudopotential calculations have been performed on GaN and AlN in the wurtzite and zinc-blende structures. The mixed-basis approach is employed due to the localized nature of the valence charge density in these materials. In the stress calculation within the mixed-basis set, a correction term is introduced to the stress expression in order to make it consistent with the pressure given by the total-energy calculations. The lattice constants in the wurtzite structure are in good agreement with the experimental data. The band gap appears to be direct except for zinc-blende AlN, which has the conduction-band minimum at the X point. The effective mass of the electron is found to be nearly isotropic for both wurtzite GaN and AlN. The agreement of the optical Γ-phonon frequencies with the Raman experimental data is excellent for wurtzite GaN and good for wurtzite AlN, except for A_1–transverse-optical (A_1-TO) mode. The calculated A_1-TO mode frequency of AlN is 11% smaller than the experimental value. Both GaN and AlN are found to have the wurtzite structure in the ground state.

I. INTRODUCTION

Gallium nitride (GaN) and aluminum nitride (AlN) are two of the most promising wide-band-gap III-V semiconductors for short-wavelength optoelectronic devices. Recently, an efficient blue light-emitting diode has been developed using Si-doped GaN.[1] Aluminum nitride has been considered to be significant, as well as the mixed compound $Al_xGa_{1-x}N$, for the development of a short-wavelength laser. However, it is difficult to grow high-quality single crystals of these materials. The experimental data often have some variations, depending on the crystal-growth condition. Therefore, it is important to understand the bulk properties of these materials from the theoretical point of view for various applications.

Over the past decade, first-principles calculations based on the density-functional theory[2] with the local-density approximation[3] (LDA) have been developed and made the accurate prediction of the ground-state properties of solids available. Although several LDA calculations have been published for GaN (Refs. 4–7) and AlN,[8,9] few studies have been done on their vibrational property. In this paper, we have performed a first-principles pseudopotential calculation on GaN and AlN to predict their fundamental properties including the optical Γ-phonon frequencies.

At the ambient conditions, GaN and AlN crystallize in the hexagonal wurtzite structure (WZ). The wurtzite semiconductors are sometimes closely related to the cubic zinc-blende (ZB) semiconductors. Although GaN and AlN are known to be highly stable in WZ, cubic GaN has been recently observed on the GaAs substrate.[10] In addition, for the crystal structure of GaN in the ground state, the results of the previous calculations[4,11] contradict each other, which give the total-energy difference between WZ and ZB with opposite signs. From these reasons, we also consider the ZB structure and the results are compared with those in the WZ structure.

The rest of this paper is organized as follows: In Sec. II, the computational procedure is described. Section III presents several tests for the accuracy, and the results and discussions are given in Sec. IV. Section V summarizes the main results of this study.

II. METHOD

The present calculations are based on the local-density-functional theory and the norm-conserving pseudopotential technique. The pseudopotentials are generated using Hamann-Schlüter-Chiang scheme[12] and fitted to analytic functions according to the method of Bachelet, Hamann, and Schlüter.[13] For gallium, the scalar relativistic effect is included. The Wigner interpolation formula[14] for the exchange-correlation energy is used both in the atomic and crystalline calculations.

Since the p pseudopotential of nitrogen is very deep due to the lack of p electrons in the core, the conventional plane-wave calculation demands much computational effort: A large number of plane waves are required to expand the electronic wave functions. Therefore, we have adopted the mixed-basis approach[15] which is very efficient for the system containing both highly localized and delocalized electrons. For each $\mathbf{k}$ in the Brillouin zone, the electronic wave functions are expressed by a linear combination of plane waves and Bloch sums of localized functions,

$$\Psi_i(\mathbf{k},\mathbf{r})=\frac{1}{\sqrt{V}}\sum_{\mathbf{G}} C_i(\mathbf{k}+\mathbf{G})e^{i(\mathbf{k}+\mathbf{G})\cdot\mathbf{r}}+\sum_n D_{in}(\mathbf{k})\phi_n(\mathbf{k},\mathbf{r}) , \tag{1}$$

where

$$\phi_n(\mathbf{k},\mathbf{r})=\frac{1}{\sqrt{V}}\sum_{\mathbf{R}} e^{i\mathbf{k}\cdot(\mathbf{R}+\tau_n)} f_n(\mathbf{r}-\mathbf{R}-\tau_n) , \quad (2)$$

C_i and D_{in} are the expansion coefficients, $\mathbf{G}$ is a reciprocal-lattice vector, $\mathbf{R}$ is a lattice vector, V is the crystal volume, and n is a label for the function and atom (located at τ_n). For the localized function, we use a single Gaussian orbital on each nitrogen site,

$$f_m(\mathbf{r})=Are^{-\lambda r^2}Y_{1m}(\theta,\varphi) , \quad (3)$$

where A is a normalization constant and $Y_{1m}(\theta,\varphi)$ are the $l=1$ spherical harmonics. The Gaussian exponent λ should be determined so as to minimize the total energy E_{tot} for a fixed set of plane waves. In order to optimize λ, it is convenient to evaluate $\partial E_{\text{tot}}/\partial\lambda$, which is given by

$$\frac{\partial E_{\text{tot}}}{\partial\lambda}=2\sum_{\mathbf{k},i} w_i \text{Re}\left[\sum_n D_{in}^*\left\langle\frac{\partial\phi_n}{\partial\lambda}\middle| H-\varepsilon_i\middle|\Psi_i\right\rangle\right] , \quad (4)$$

where w_i is the occupation number, H and ε_i are the self-consistent single-electron Hamiltonian and its eigenvalues, respectively, and the index i goes over all the occupied valence states.

The evaluation of the atomic force and the macroscopic stress helps in finding the stable atomic configuration, in particular when the crystal structure has low symmetry like the WZ structure. In the force calculation within the mixed-basis set, the incomplete basis set correction[16] to Hellmann-Feynman force must be taken into account because the localized Bloch functions depends on atomic positions.

The macroscopic stress can be calculated from the stress theorem proposed by Nielsen and Martin[17] and they have derived the reciprocal-space expression of the stress.[18] In the mixed-basis approach, the localized Bloch functions are expanded in plane waves and the electronic wave functions are then given in a Fourier representation. Hence, the stress expression within the mixed-basis set can be obtained by substituting

$$\Psi_i(\mathbf{k}+\mathbf{G})=\frac{1}{\sqrt{V}}\left[C_i(\mathbf{k}+\mathbf{G})+\sum_n D_{in}(\mathbf{k})e^{-i\mathbf{G}\cdot\tau_n}f_n(\mathbf{k}+\mathbf{G})\right] \quad (5)$$

in the original plane-wave expression, Eq. (2) of Ref. 18, where $f_n(\mathbf{k}+\mathbf{G})$ is the Fourier transform of the localized function.

There is, however, a problem in determining the pressure using the stress calculation. The Gaussian exponent λ optimized at a specific volume is usually kept fixed when the pressure is evaluated from the total-energy calculations. On the other hand, the stress calculation takes the derivative of the total energy with respect to volume by applying the scaling procedure which leads to the transform of λ into $(1+\epsilon)^{-2}\lambda$, where ϵ is a hydrostatic strain. In order to overcome this ambiguity, we have introduced a correction term to the stress expression. The change in the total energy due to scaling λ is given by

$$\frac{\partial E_{\text{tot}}}{\partial\lambda}\frac{\partial\lambda}{\partial V}=-\frac{2\lambda}{3V}\frac{\partial E_{\text{tot}}}{\partial\lambda} , \quad (6)$$

which brings the ambiguity of the pressure. Thus, the stress expression within the mixed-basis set is obtained by subtracting this term from the reciprocal-space expression of the stress:

$$\sigma_{\alpha\beta}=\frac{1}{V}\frac{\partial E_{\text{tot}}}{\partial\epsilon_{\alpha\beta}}+\frac{2\lambda}{3V}\frac{\partial E_{\text{tot}}}{\partial\lambda}\delta_{\alpha\beta} , \quad (7)$$

where the first term is the stress obtained from the reciprocal-space expression and the second term indicates the pressure correction for scaling λ, which is analytically calculated from Eq. (4). When the Gaussian exponent λ is sufficiently optimized for a given set of plane waves, the correction term becomes negligible because $\partial E_{\text{tot}}/\partial\lambda\simeq 0$.

In this study, the constant number of plane waves is used to introduce a cutoff on plane waves. The number of plane waves is kept fixed at 2189 for WZ and 1067 for ZB. The corresponding cutoff energy E_{cut} is about 28 hartrees. The Brillouin-zone $\mathbf{k}$ integration is performed by the special-points method of Chadi and Cohen[19] and Monkhorst and Pack.[20] We use six special $\mathbf{k}$ points for WZ and two special $\mathbf{k}$ points for ZB, or the equivalent in the irreducible Brillouin zone, unless otherwise noted. The optimum value of the Gaussian exponent is obtained as $\lambda_{\text{opt}}=4.08$ a.u.$^{-2}$ for ZB-GaN and this value is also employed for other cases; we have found that $\partial E_{\text{tot}}/\partial\lambda$ is held small throughout this work, which ensures the high quality of the value of λ.

III. EXAMINATION

We have carried out three kinds of tests for accuracy. First, we have compared the pressure P_{stress} given by Eq. (7) with the pressure P_{TE} derived from the total energy curve to confirm the validity of the stress calculation within the mixed-basis set. The calculation is performed on ZB-GaN. The number of plane waves is fixed for the consistency of P_{TE} and P_{stress}.[21] Murnaghan's equation of state is used for determining P_{TE}. The Gaussian exponent $\lambda=3.8$ a.u.$^{-2}$ is chosen instead of $\lambda_{\text{opt}}=4.08$ a.u.$^{-2}$ to examine the correction term in Eq. (7). The excellent agreement between P_{TE} and P_{stress} is obtained as shown in Table I. Since the value of λ is not the optimized one, the pressure correction is not negligible. This

TABLE I. Comparison of pressure given by the total-energy calculation (P_{TE}) and the stress calculation (P_{stress}) for ZB-GaN. The last column gives the second term of Eq. (7).

a (Å)	P_{TE} (GPa)	P_{stress} (GPa)	Correction (GPa)
4.40	6.22	6.21	−0.64
4.42	3.29	3.28	−0.68
4.44	0.53	0.52	−0.73
4.46	−2.07	−2.08	−0.77
4.48	−4.52	−4.53	−0.81
4.50	−6.82	−6.83	−0.85

term works well to correct the pressure given by the reciprocal-space expression of the stress. Additional information can be found in this calculation. The lattice constant a and bulk modulus B calculated here are 4.444 Å and 196 GPa, respectively, which are very close to those obtained using λ_{opt} (see Table II). As discussed in Ref. 15, the results are insensitive to the value of λ.

Second, a comparison between the mixed-basis approach and the plane-wave approach has been made. Figure 1 shows the pressure P of ZB-GaN at $a=4.44$ Å as a function of the cutoff energy E_{cut}. The fully converged values of P given by the two approaches agree within 0.5 GPa. The pressure convergence is within 0.6 GPa with our basis set (shown by an arrow in Fig. 1), whereas the same level of convergence with the plane-wave basis set requires a large cutoff energy, $E_{cut}=56$ hartrees. This means that the number of plane waves required is about three times larger than that in our basis set. Assuming the linear relation $\Delta a/a=-\Delta P/(3B)$, the uncertainty in a introduced by the convergence error ΔP is expected to be 0.1% in our basis set. We also consider the nonisotropic deformation. The shear stress $\sigma_{xx}-\sigma_{yy}$ is evaluated with the uniaxial strain of $\epsilon_{xx}=0.02$, and is predicted as 2.99 GPa within the mixed-basis set and 3.00 GPa within the plane-wave basis set. The two calculations give almost same value. From these results, we can conclude that the mixed-basis approach is as accurate as the plane-wave approach.

Finally, the convergence test has been performed with respect to the Brillouin-zone **k**-point sampling. In going to denser **k**-point mesh, the change in P is below 0.2 GPa for ZB-GaN and 0.1 GPa for WZ-GaN.

IV. RESULTS AND DISCUSSION

For the WZ structure, the equilibrium structural parameters, the lattice constant a, axial ratio c/a, and internal parameter u, are determined so that the forces on atoms along the c axis, F_z, and the diagonal elements of the stress tensor, $\sigma_{xx}=\sigma_{yy}$ and σ_{zz}, vanish. For the ZB structure, unlike the WZ case, the structural parameter is only the lattice constant a and its equilibrium value is obtained from the condition that pressure is equal to zero. The bulk modulus B can be obtained from the numerical volume derivative of the pressure around the equilibrium volume. We apply ±1% variations in volume, assuming that c/a and u are fixed at the equilibrium values for WZ.

TABLE II. Lattice constants a, axial ratios c/a, internal parameters u, and bulk moduli B.

	GaN		AlN	
	Calc.	Expt.[a]	Calc.	Expt.[b]
	Wurtzite structure			
a (Å)	3.146	3.189	3.144	3.112
c/a	1.629	1.626	1.605	1.600
u	0.377		0.381	
B (GPa)	195		194	
	Zinc-blende structure			
a (Å)	4.446		4.421	
B (GPa)	195		195	

[a]Reference 22.
[b]Reference 23.

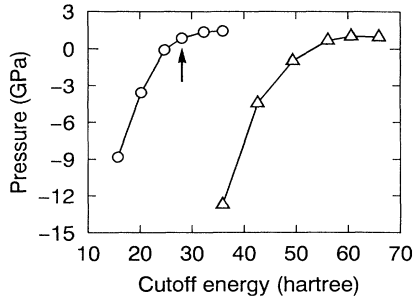

FIG. 1. Pressure of ZB-GaN at lattice constant $a=4.44$ Å as a function of the cutoff energy. Circles are the calculated pressure within the mixed-basis set ($\lambda=4.08$ a.u.$^{-2}$) and triangles are within the plane-wave basis set. The arrow indicates the basis set used for the zinc-blende structure in this work.

Table II shows the results of the calculation, together with the experimental data. The agreement with experimental data is very good, though it should be noted that some variations of the experimental data have been found in other literature.[24] The structure of WZ-GaN is close to the ideal WZ structure in which $c/a=\sqrt{8/3}\simeq 1.633$ and $u=0.375$, while large relaxation from the ideal WZ structure is found for WZ-AlN with a smaller c/a and a larger u than the ideal values. The difference in lattice constant between WZ-GaN and WZ-AlN is 0.1% along the a axis and 1.5% along the c axis. This small lattice mismatch opens the possibility of growing the mixed compound $Al_xGa_{1-x}N$. The bulk moduli of WZ-GaN and WZ-AlN are almost equal. We can expect that the errors in B introduced by the assumption of the ideal isotropic deformation are negligible because the shear stress $\sigma_{xx}-\sigma_{zz}$ and forces on atoms F_z are still small under this deformation. This implies small elastic anisotropy of WZ-GaN and WZ-AlN. The lattice constants of ZB-GaN and ZB-AlN are quite close to the expected ones (4.445 and 4.421 Å, respectively) obtained by assuming that they have the same atomic volume in the WZ structure. The bulk modulus of ZB-GaN and ZB-AlN is also very close to that in the WZ structure. The lattice mismatch in the ZB case is 0.6%.

The valence charge contour plots for GaN in the WZ and ZB structure are shown in Figs. 2(a) and 2(b), respectively. The charge plotted is normalized to the average valence charge density of the unit cell. There is no remarkable difference between the plots for WZ and ZB, except for the bonding direction. As expected, the valence charge densities of WZ-GaN and ZB-GaN are strongly localized around nitrogen; the maximum charge density is about ten times larger than the average charge density. The charge distribution around nitrogen is almost spherical and the bonding character seems to be ionic rather than covalent. The valence charge contour plots for AlN are given in Fig. 3. For both the WZ and ZB cases, the charge density of AlN is similar to that of GaN, but the valence charge is slightly more localized for AlN than for GaN. For better comparison, the charge

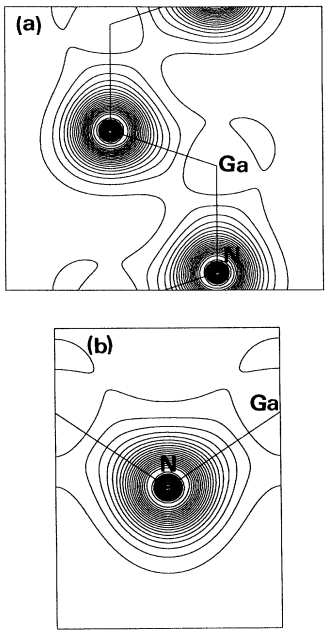

FIG. 2. Valence charge contour plots for (a) WZ-GaN in the (100) plane and (b) ZB-GaN in the $(1\bar{1}0)$ plane. The charge plotted is normalized to the average valence charge density of the unit cell. The contour spacing is 0.5 and the bonding directions are illustrated by the straight lines.

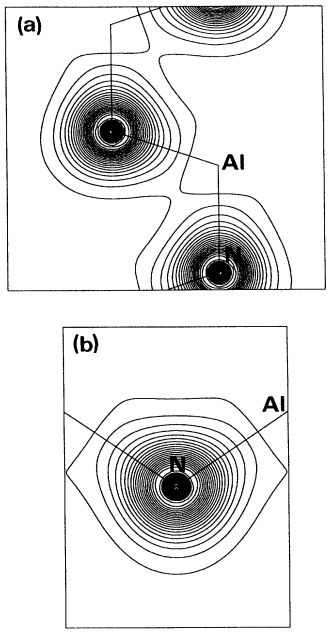

FIG. 3. Valence charge contour plots for (a) WZ-AlN in the (100) plane and (b) ZB-AlN in the $(1\bar{1}0)$ plane. See caption of Fig. 2.

difference between ZB-GaN and ZB-AlN is plotted in Fig. 4. This figure illustrates that more charge is transferred to around nitrogen for AlN, most of which is accumulated in the off-bond region. This makes the bonding of AlN more ionic. The corresponding plot for the WZ case is not meaningful due to the displacement of the sublattice (different u as shown in Table II). Comparing the charge densities in the ideal WZ structure, we have obtained a plot similar to Fig. 4.

Figure 5(a) depicts the electronic band structure of WZ-GaN. The band gap of WZ-GaN is found to be direct. The calculated size of the band gap, $E_g^{\mathrm{LDA}}=2.89$ eV, is smaller than the experimental value of 3.4 eV. Although it is widely known that the LDA calculation usually underestimates the size of the band gap, we can expect that it has enough accuracy to determine whether the band gap is direct or not and gives fairly good results for the band-energy dispersion. The effective-mass components of the electron derived from the LDA calculations are $m_{\parallel}^{*}=0.20m_0$ along the Γ-A symmetry line and $m_{\perp}^{*}=0.22m_0$ perpendicular to that. The experimental value is $0.20m_0$.[25] The electronic band structure of WZ-AlN is shown in Fig. 6(a). The band gap is direct with $E_g^{\mathrm{LDA}}=4.09$ eV, which is smaller than the experimental value of 6.3 eV, and the effective mass predicted is $m_{\parallel}^{*}=0.29m_0$ and $m_{\perp}^{*}=0.30m_0$. Our results suggest that the effective mass of the electron of WZ-GaN and WZ-AlN has a small dependence on the direction of $\mathbf{k}$. The band structure of ZB-GaN and ZB-AlN are given in Figs. 5(b) and 6(b), respectively. The plot for ZB-GaN shows that the energy band gap is direct with $E_g^{\mathrm{LDA}}=2.73$ eV and $m^{*}=0.21m_0$. For ZB-AlN, the band gap appears to be indirect with $E_g^{\mathrm{LDA}}=3.07$ eV at the X point and the effective mass of the electron is predicted as $m_l^{*}=0.51m_0$ and $m_t^{*}=0.31m_0$.

The optical Γ-phonon frequencies are obtained by solving the secular equation for the dynamical matrix. The dynamical matrix is numerically constructed by calculating forces on atoms with small displacement of an atom. The displacement is taken as ± 0.01 Å. The results are listed in Table III. The agreement with the Raman experimental data is excellent for WZ-GaN. The calculated frequencies of WZ-AlN agree well with the Raman experimental data except for the A_1-transverse-optical (TO) mode. The calculated A_1-TO mode frequency of WZ-AlN is 11% smaller than the experimental value. We be-

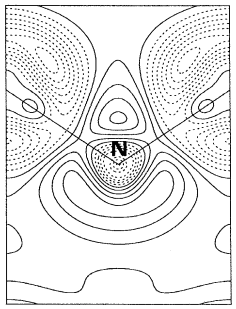

FIG. 4. Charge difference between ZB-AlN and ZB-GaN in the $(1\bar{1}0)$ plane. The function plotted is the normalized density of ZB-AlN minus that of ZB-GaN. The contour spacing is 0.01 and the dashed contours correspond to negative values.

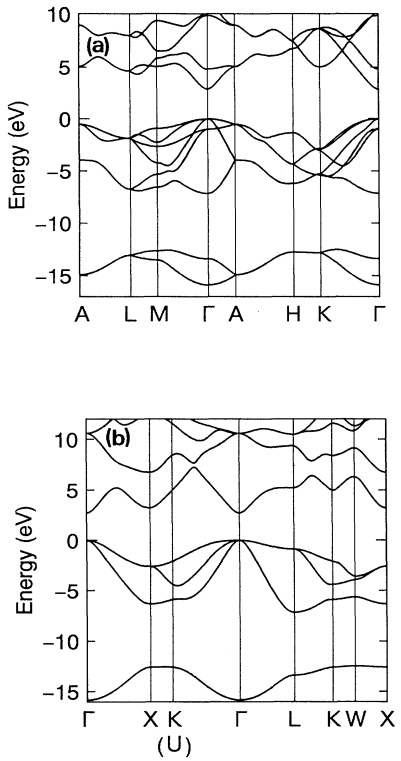

FIG. 5. Energy band structures of (a) WZ-GaN and (b) ZB-GaN. The origin of the energy is set at the top of the valence band.

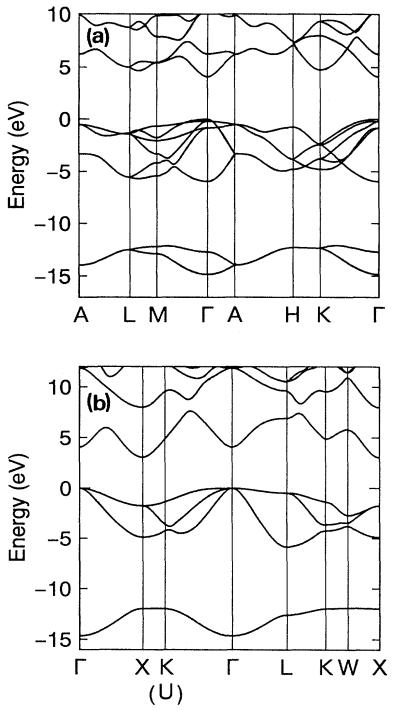

FIG. 6. Energy band structures of (a) WZ-AlN and (b) ZB-AlN. The origin of the energy is set at the top of the valence band.

lieve that this discrepancy is much larger than the uncertainties in our calculations. In Fig. 1(a) of Ref. 27, we can find an extremely strong band at 610 cm^{-1} which agrees well with our result, although the authors have concluded that this band is not due to a first-order Raman process. In connection with this discrepancy, more detailed investigations will be needed.[28]

The TO-phonon frequency in the ZB structure is very close to the E_1-TO mode frequency in the WZ structure for both GaN and AlN. In our calculation, the longitudinal vibration frequencies cannot be obtained for the infrared-active modes since they have contributions from the macroscopic electric field. Although the supercell method[29] is capable of overcoming this, it is computationally impractical in our system.

In order to determine the crystal structure in the ground state for GaN and AlN, the total-energy calculations are performed with the denser **k**-point mesh. We use 12 special **k** points for WZ and 28 special **k** points for ZB. The convergence test indicates that the errors in total energy with respect to the **k**-point sampling and the plane-wave cutoff energy are less than 1 meV. From comparison of the total energies, we confirm that GaN and AlN have the WZ structure in the ground state. The energy difference between WZ and ZB is 5.8 meV/atom for GaN and 18.7 meV/atom for AlN. These values are in good agreement with the ones in the previous calculation by Yeh *et al.*[11]

V. SUMMARY

We have performed a first-principles pseudopotential calculation on GaN and AlN. The mixed-basis approach is adopted due to the localized nature of the valence charge density in these materials. The calculation of the atomic force and the macroscopic stress is utilized to predict their properties. In the stress calculation within the mixed-basis set, we have introduced the pressure correction to the original reciprocal-space expression of the stress in order to make the results consistent with those provided by the total-energy calculations. Our examinations indicate that the mixed-basis approach is more efficient for the system containing the localized com-

TABLE III. Optical Γ-phonon frequencies in units of cm^{-1}.

	GaN		AlN	
	Calc.	Expt.[a]	Calc.	Expt.[b]
		Wurtzite structure		
A_1-TO	534	531	601	667
B_1	335	inactive	534	inactive
B_1	697	inactive	703	inactive
E_1-TO	556	560	650	667
E_2	146	144	228	
E_2	560	568	638	655
		Zinc-blende structure		
TO	558		648	

[a]Reference 26.
[b]Reference 27.

ponents than the conventional plane-wave approach, retaining high accuracy. It should be noted that the efficiency of the mixed-basis approach may decrease with increasing number of localized functions in the basis set, since the correction terms for the atomic force and the stress become dominant in the computing time.

In conclusion, we have predicted the equilibrium structural parameters, bulk moduli, electronic band structures, and optical Γ-phonon frequencies of GaN and AlN in the wurtzite and zinc-blende structures. The lattice constants of WZ-GaN and WZ-AlN are in good agreement with the experimental data. The electronic band structures given by LDA suggest that WZ-GaN and WZ-AlN have nearly isotropic effective mass of the electron. The agreement of the optical Γ-phonon frequencies with the Raman experimental data is excellent for WZ-GaN and for WZ-AlN except for the A_1-TO mode. The calculated A_1-TO mode frequency of WZ-AlN shows the difference of 11% from the experimental value. Both GaN and AlN are found to have the WZ structure in the ground state.

ACKNOWLEDGMENTS

We wish to thank Dr. H. Hayashi for many helpful discussions. We also wish to thank Mr. T. Kozawa and Mr. T. Sugiyama for informing us of experimental details.

[1]N. Koide, H. Kato, M. Sassa, S. Yamasaki, K. Manabe, M. Hashimoto, H. Amano, K. Hiramatsu, and I. Akasaki, J. Cryst. Growth **115**, 639 (1991).
[2]P. Hohenberg and W. Kohn, Phys. Rev. **136**, B864 (1964).
[3]W. Kohn and L. J. Sham, Phys. Rev. **140**, A1133 (1965).
[4]B. J. Min, C. T. Chan, and K. M. Ho, Phys. Rev. B **45**, 1159 (1992).
[5]A. Muñoz and K. Kunc, Phys. Rev. B **44**, 10 372 (1991).
[6]P. Perlin, I. Gorczyca, N. E. Cristensen, I. Grzegory, H. Teisseyre, and T. Suski, Phys. Rev. B **45**, 13 307 (1992).
[7]P. E. Van Camp, V. E. Van Doren, and J. T. Devreese, Solid State Commun. **81**, 23 (1992).
[8]W. Y. Ching and B. N. Harmon, Phys. Rev. B **34**, 5305 (1986).
[9]P. E. Van Camp, V. E. Van Doren, and J. T. Devreese, Phys. Rev. B **44**, 9056 (1991).
[10]M. Mizuta, S. Fujieda, Y. Matumoto, and T. Kawamura, Jpn. J. Appl. Phys. **25**, L945 (1986).
[11]C.-Y. Yeh, Z. W. Lu, S. Froyen, and A. Zunger, Phys. Rev. B **45**, 12 130 (1992); **46**, 10 086 (1992).
[12]D. R. Hamann, M. Schlüter, and C. Chiang, Phys. Rev. Lett. **43**, 1494 (1979).
[13]G. B. Bachelet, D. R. Hamann, and M. Schlüter, Phys. Rev. B **26**, 4199 (1982).
[14]E. Wigner, Phys. Rev. **46**, 1002 (1934).
[15]S. G. Louie, K.-M. Ho, and M. L. Cohen, Phys. Rev. B **19**, 1774 (1979).
[16]P. Bendt and A. Zunger, Phys. Rev. Lett. **50**, 1684 (1983).
[17]O. H. Nielsen and R. M. Martin, Phys. Rev. B **32**, 3780 (1985).
[18]O. H. Nielsen and R. M. Martin, Phys. Rev. B **32**, 3792 (1985).
[19]D. J. Chadi and M. L. Cohen, Phys. Rev. B **8**, 5747 (1973).
[20]H. J. Monkhorst and J. D. Pack, Phys. Rev. B **13**, 5188 (1976).
[21]P. G. Dacosta, O. H. Nielsen, and K. Kunc, J. Phys. C **19**, 3163 (1986).
[22]H. P. Maruska and J. J. Tietjen, Appl. Phys. Lett. **15**, 327 (1969).
[23]W. M. Yim and R. J. Paff, J. Appl. Phys. **45**, 1456 (1974).
[24]For example, O. Lagerstedt, and B. Monemar, Phys. Rev. B **19**, 3064 (1979).
[25]A. S. Barker, Jr. and M. Ilegems, Phys. Rev. B **7**, 743 (1973).
[26]P. Perlin, C. Janberthie-Carillon, J. P. Itie, A. S. Miguel, I. Grzegory, and A. Polian, Phys. Rev. B **45**, 83 (1992).
[27]O. Brafman, G. Lengyel, and S. S. Mitra, Solid State Commun. **6**, 523 (1968).
[28]Very recently, the Raman experimental data of AlN, which agree well with our results, have been published by P. Perlin, A. Polian, and T. Suski, Phys. Rev. B **47**, 2874 (1993).
[29]K. Kunc and R. M. Martin, Phys. Rev. Lett. **48**, 406 (1982).